Strain relief at the GaSb/GaAs interface versus substrate surface treatment and AlSb interlayer thickness

Y. Wang, P. Ruterana, L. Desplanque, S. El Kazzi, X. Wallart

Strain relief at the GaSb/GaAs interface versus substrate surface treatment and AlSb interlayers thickness

Cite as: J. Appl. Phys. **109**, 023509 (2011); https://doi.org/10.1063/1.3532053
Submitted: 02 September 2010 • Accepted: 01 December 2010 • Published Online: 19 January 2011

Y. Wang, P. Ruterana, L. Desplanque, et al.

Strain relief at the GaSb/GaAs interface versus substrate surface treatment and AlSb interlayers thickness

Y. Wang,[1,a)] P. Ruterana,[1] L. Desplanque,[2] S. El Kazzi,[2] and X. Wallart[2]
[1]*CIMAP, UMR 6252, CNRS-ENSICAEN-CEA-UCBN, 6, Boulevard du Maréchal Juin, 14050 Caen Cedex, France*
[2]*UMR-CNRS 8520, Institut d'Electronique, de Microélectronique et de Nanotechnologie, UMR-CNRS 8520, BP 60069, 59652 Villeneuve d'Ascq Cedex, France*

(Received 2 September 2010; accepted 1 December 2010; published online 19 January 2011)

Using transmission electron microscopy we investigate the influence of AlSb monolayers and substrate surface preparation on the microstructure of GaSb grown on GaAs (001) by molecular beam epitaxy. The geometric phase analysis method is used to analyze the interface dislocation type and the residual strain, as well as the dislocation core behavior versus the thickness of the AlSb interface layer. A quantitative measurement of the local Burgers vectors shows that the misfit dislocations at the GaSb/GaAs interface are always 60° dislocations. They are arranged in pairs which are more or less distant. For the samples with the lower threading dislocation density, the average distance between the 60° pairs is smaller, the interface is flatter and the local strain is more relieved. These results show that understanding the atomic structure of interfaces may be of great help in improving the quality of GaSb grown on GaAs substrates. © *2011 American Institute of Physics*. [doi:10.1063/1.3532053]

I. INTRODUCTION

Metamorphic epitaxy of high lattice-mismatch Sb-based materials on GaAs is attracting much attention for potential applications in electronic and optoelectronic devices due to their unique band-structure alignments, small electron effective mass and high electron mobility.[1–3] With the large mismatch (7.8%) between GaSb and GaAs, the critical thickness is expected to be within the range of a few monolayers (MLs) and the growth mode should theoretically correspond to the three-dimensional (3D) Volmer–Weber with formation of relaxed islands[4] which subsequently coalesce to give rise to the epilayer.[5] The classical mechanism of relaxation should be the generation of 60° dislocations at island surface, followed by their glide to the interface and subsequent reaction to form 90° Lomer dislocations which should be the most efficient defects for the strain relief.[6,7] This growth mode has been largely investigated during the past decades and one of the representatives has been the GaAs/Si for optoelectronic integration in the Si technology.[8] In these reports, both 90° and 60° misfit dislocations were present at the interfaces subsequent to the island coalescence.[9–11] Afterwards, many parameters govern the crystalline quality of the epitaxial layer, some of them are the island size distribution, their state of relaxation (number and type of underlying misfit dislocations), mutual islands orientation, etc. Such parameters are not easily controlled, they are expected to depend on the mismatch between the epitaxial layer and the substrate, the growth conditions (temperature, method, growth kinetics, and surfactants).

Early reports showed that low strain systems $<2\%$ resulted in 60° dislocations, moderate strain (3%–4%) in mixed Lomer and 60° dislocations, and high strain $>6\%$ in pure Lomer.[12] It has also been shown that the growth temperature strongly determines the type of misfit dislocations which is produced, with GaSb grown at 520 °C giving rise to 90° misfits and 560 °C favoring 60° dislocations.[13,14] Recently, it was claimed that particular growth conditions can be tuned for the formation of 90° rather than 60° misfits dislocations, which seems to require balancing of strain energy with adatom migration, Sb overpressure, and growth temperature. A demonstration was provided for a highly periodic array of 90° misfit dislocation based growth of GaSb on GaAs to yield almost completely (~98%) relaxed and low dislocation density in the GaSb layers on GaAs ($\sim 10^5$ cm^{-2}). Interestingly, a such low dislocation density was attained subsequent to a planar growth mode established after only 3 ML of GaSb.[15] Using this optimized growth mode, laser emission in the infrared has been recently demonstrated.[16]

In the same vein, several research groups have reported that the insertion of AlSb interfacial MLs should be able to improve GaSb layer quality on various substrates, such as Si (Refs. 17–19) and GaAs,[20,21] with a suggested better relief of the strain for the smallest AlSb thickness.[21,22] Although these studies are of interest for understanding the role of AlSb buffer, few reports were issued on the atomic structure of the interfaces, and any is hardly available on the strain relaxation at the nanometer scale taking into account the types of the misfit dislocations.

In this work, transmission electron microscopy (TEM) has been used to investigate the microstructural properties of the GaSb grown on GaAs substrates following the insertion of a few MLs of AlSb at the interface. Specifically, High Resolution TEM (HRTEM) in combination with the geometrical phase analysis (GPA) method is used to analyze the interface dislocations behavior versus the thickness of the AlSb interlayer and GaAs surface preparation.

a)Electronic mail: yi.wang@ensicaen.fr.

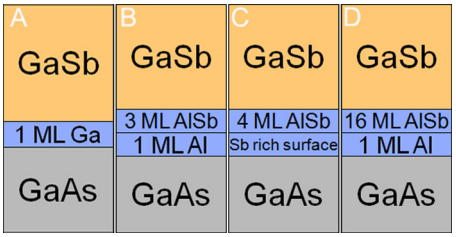

FIG. 1. (Color online) Schematic diagrams of the lay out of the four investigated samples

II. EXPERIMENTAL PROCEDURES

The investigated four GaSb layers were grown on GaAs (001) ±0.5° semi-insulating substrates by molecular beam epitaxy in a 3 in. Riber Compact 21TM reactor with a base pressure better than 1×10^{-10} Torr. After deoxidation at 625 °C under an As flux, a 500 nm GaAs layer was first grown at 580 °C to smooth the surface. Then the As valve was closed and the sample temperature was decreased to 510 °C under Sb_2 flux for sample C and without any flux for samples A, B, and D. For these latter samples, we waited until the reactor pressure has reached the 10^{-9} Torr range before continuing the growth. For samples B and D, an AlSb layer was inserted between the GaAs buffer and the GaSb layer. We started by depositing 1 ML Al followed by 3 ML AlSb (sample B) and 16 ML AlSb (sample D). For sample A, we deposited 1 ML Ga before growing the GaSb layer. For sample C, 4 ML AlSb were inserted between the GaAs buffer and GaSb layer. The growth rate was 0.7 ML/s for the antimonide layers; the growth process was monitored by *in situ* reflection high-energy electron diffraction (RHEED). The Sb_2 exposure during cooling of the GaAs buffer leads to a (2×8) RHEED pattern whereas for the other samples the starting reconstruction was (2×4). During the initial steps, the RHEED pattern turned rapidly to a 3D RHEED pattern indicative of a Volmer–Weber mode when AlSb or GaSb growth began. After a few nanometers, we recovered a two-dimensional RHEED pattern with 1×3 surface reconstruction. The GaSb layer thickness was 600 nm, the structure of the samples is schematically shown in Fig. 1.

The sample preparation for TEM was achieved using conventional mechanical polishing and dimpling with a final step of ion milling. The argon ion milling was performed at −150 °C to minimize ion damage. The samples were observed in two JEOL microscopes: a 2010 FEG for HRTEM analysis and a 2010LaB_6 for conventional TEM both operated at 200 kV.

III. RESULTS

Cross-sectional, plan view, and HRTEM investigations were made in order to analyze the interface dislocations, the AlSb interlayers and the resulting GaSb crystalline quality. Figures 2(a) and 2(b) show the cross-sectional micrographs of samples B and D, respectively. As can be noticed, threading dislocations are generated at the interface between the GaSb epitaxial layer and GaAs substrate, some of them cross the whole epitaxial layer, whereas others had their lines cut during the sample preparation. Such observation cannot be

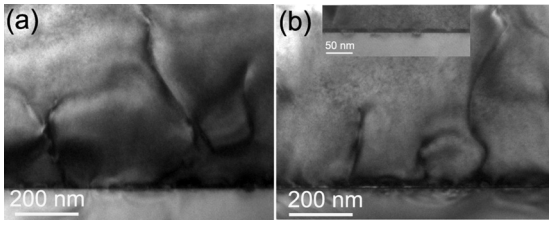

FIG. 2. Cross-sectional bright-field TEM images of sample B and D. The inset in (b) is a enlarge view of the interface showing the morphology of AlSb buffer.

used to state that the dislocation density decreases with the increase in the epitaxial layer thickness. In addition, as the dislocations have a/2 ⟨110⟩ Burgers vectors some of them will be out of contrast in observations carried out in cross sections along ⟨110⟩ type zone axis. Therefore, in order to determine the dislocation density, we have carried out plan view observations along the [001] zone axis. Indeed, it may also be taken into account that a reduction in dislocation density may occur due to interactions and annihilations which take place mostly close to the interface with the substrate where the density is still very high. Another important feature of Fig. 2(b) needs to be pointed out: the contrast at the interface reveals the morphology of the AlSb interlayer, especially for sample D as shown in the inset of Fig. 2(b) where the layer is clearly delineated and continuous.

Figure 3 shows plan view TEM micrographs of sample B and C: the threading dislocations appear as dark dots/lines on the shiny GaAs background. The averaged threading dislocations estimated from more than ten images for each sample are summarized in Table I, i.e., 8×10^8, 9×10^8, 6×10^7, and 7×10^8 threading dislocations/cm^2 for samples A, B, C, and D, respectively. Obviously, sample C, for which the 4 ML AlSb growth was initiated on a Sb-rich GaAs surface, exhibits the lowest threading dislocation density and the others almost stay in the same level. An interesting question is if this comes from a particular atomic structure at the interface. Indeed, it has been claimed that the formation of misfit arrays of Lomer dislocations contribute to strongly decrease the threading dislocation densities.[3,15,22] In order to check this, we have carried out a detailed HRTEM analysis of these samples; the results are discussed in the next sections.

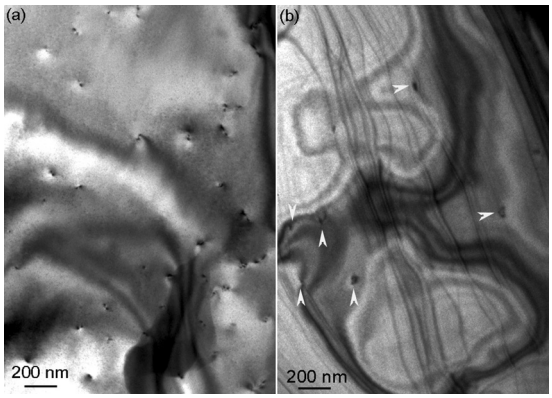

FIG. 3. Plan view TEM images of sample B and C, recorded close to the [001] growth axis.

TABLE I. Interface structure data for the investigated samples.

	Sample A	Sample B	Sample C	Sample D
Layers of AlSb (ML)	0	3	4	16
Threading dislocation (10^8 defects/cm^2)	8 ± 2	9 ± 1	0.6 ± 0.1	7 ± 2
60° dislocation (%)	10	17.4	0	5.6
Spacing of Lomer (nm)	5.7 ± 0.2	5.3 ± 0.7	5.5 ± 0.1	5.6 ± 0.3
Thickness of interface (nm)	2.12	2.02	0.70	1.14
Pure Lomer dislocation (%)	64.7	68.4	100	75.8

In Fig. 4, HRTEM images of the interfaces between the buffer layers and the GaAs (001) substrates for sample A [Fig. 4(a)] without AlSb interlayer and sample B with 4 ML of AlSb are exhibited. These micrographs have been recorded along the [110] direction; the positions of the interface dislocations have been marked by the additional {111} lattice planes. With their [110] Burgers vector, Lomer dislocations are characterized by two additional lattice planes, whereas the 60° have a/2 [101] Burgers and only one additional {111} lattice plane. The extra half planes of the misfit dislocations are observed in the GaAs substrate because the lattice constant of GaSb is larger than that of the GaAs substrate. If we take the interface as the line which is defined by the location of the dislocations (inclined arrows), it can be noticed that the interface in the two samples appears not completely flat, and except one well defined 60° dislocation in sample B, for the two samples, it is not obvious to locate the cores of the interface dislocations.

When the growth is initiated on the (2×8) reconstructed Sb-riched GaAs surface, as shown in Fig. 5(a) for sample C, the misfit dislocations appear to settle inside the same (001) lattice plan and the interface becomes flat. Moreover, in contrast to the other samples, at this scale, all the {111} additional lattice plane pairs of each Lomer dislocation are seen to originate from the same points. This is a clear indication that we now have compact Lomer interfacial dislocations. The investigated thickest AlSb interlayer is also interesting; as shown in Fig. 5(b), when the AlSb interlayer thickness is increased to some 16 ML (5 nm) for sample D, the interface is still flat. However, a close examination of the additional lattice planes shows that the interface dislocations are less compact than in Fig. 5(a). Confirming the TEM results as shown in Fig. 2, the AlSb layer is now continuous because of the coalescence of the AlSb islands; its limit is marked by horizontal white arrows in Fig. 5(b). As could be expected from the small mismatch between AlSb and GaSb, there are no observed misfit dislocations at the top of the AlSb interlayer. A similar behavior of insertion a thick layer AlSb was reported by Kim *et al.*;[21] although these authors have dealt with even thicker AlSb interlayers (9 and 22 nm), therefore, our observations may be pointing out to a possible degradation of the layer quality starting at smaller AlSb interlayer thickness. Based on the analysis of several images (with more than 30 pairs of dislocations for each sample), the fraction of the 60° dislocations and the mean spacing of the Lomer dislocations are summarized in Table I.

The sudden improvement from sample B to C may probably be related to a critical size effect for the AlSb islands.[23] During this initial growth stage, the AlSb deposits into coherent islands at the GaAs surface. It appears that the Sb-rich surface reconstruction promotes a better wetting of AlSb on the GaSb surface. Looking at our statistical results in Table I, the higher percentage of 60° misfit dislocations and wide

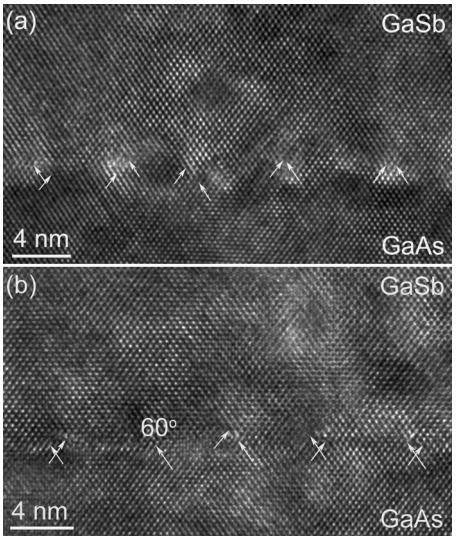

FIG. 4. HRTEM images of the buffer layer and GaAs interface along the [110] orientation, inclined arrows indicate extra {111} planes at the interface. (a) Sample A, the cores of the Lomer dislocations are extended inside the interface and in the GaSb layer, (b) sample B, the Lomer dislocation cores are extended, as well, and a pure 60° dislocation is also visible.

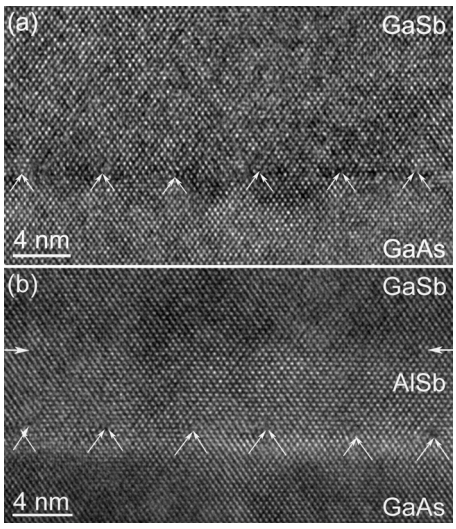

FIG. 5. HRTEM images of the buffer layer and GaAs interface along the [110] orientation. (a) Sample C, the dislocations are of Lomer-type, with compact cores. (b) Sample D, the AlSb/GaSb interface is shown by horizontal white arrows.

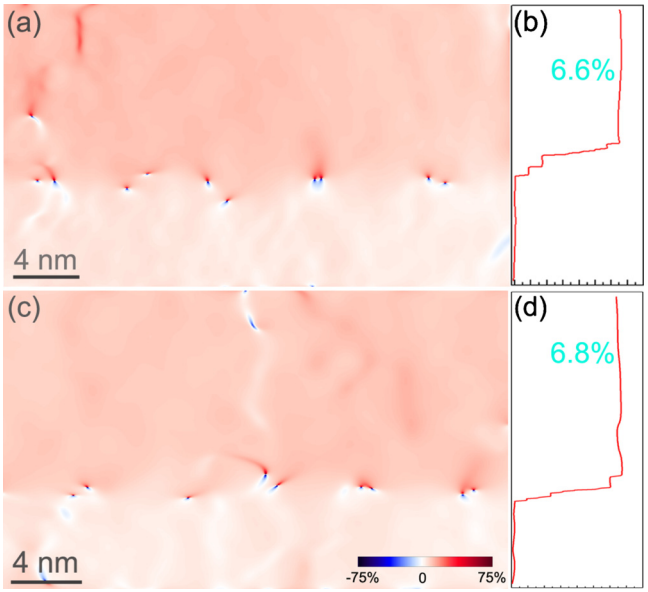

FIG. 6. (Color online) Strain components ε_{xx} images corresponding to the Fig. 3 HRTEM images, (a) sample A all the cores of the Lomer dislocations are clearly separated. (b) Projection of the ε_{xx} images on the growth direction, the broken horizontal line shows that the interfacial area is large. (c) Sample B, the interface is slightly flatter than in sample A, (d) the release of the misfit strain is also improved.

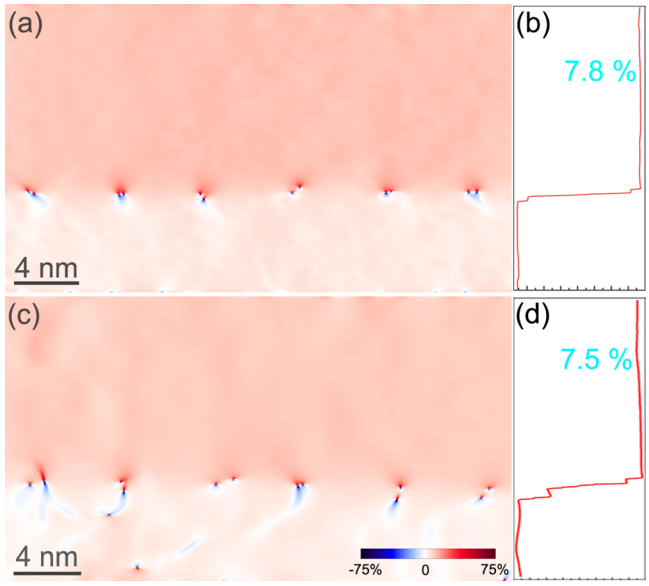

FIG. 7. (Color online) Strain components ε_{xx} images corresponding to the Fig. 4 HRTEM images, (a) In sample C the cores of the Lomer dislocations are compact. (b) Projection of the ε_{xx} images along the interface direction, the misfit strain is locally relieved. (c) Sample D, the distance between the pairs of interfacial 60° dislocation is now obvious for all the dislocations, although smaller than in samples A and B. (d) The misfit strain has been relieved up to 96%.

distribution of Lomer dislocation spacing of sample B are in agreement with such a process. The improved GaSb bulk layer quality and interface seems to be related to a larger coverage of GaAs surface by AlSb. The rougher interface and higher percentage of 60° dislocations of sample A and B originated from the larger contact area at GaSb/GaAs heterointerface. A similar phenomenon was also reported by Kim *et al.*[13] in GaSb/Si system with an AlSb buffer layer. Conventionally, the 60° dislocations which have their Burgers vector out of the interface plane are considered as possible easier sources for the threading dislocations;[24] the higher percentage of such defects in sample A and B is consistent with the density of threading dislocation obtained from the plan view observations. However, on growth of a thick AlSb layer, the AlSb islands will have coalesced into a continuous nanometric layer, as has been pointed out above in Fig. 2. As shown in Fig. 5(b) the lighter contrast at the GaAs surface corresponds to this AlSb buffer layer (the horizontal arrows indicate the interface of AlSb/GaSb). This is probably equivalent to directly grow an AlSb bulk layer on the GaAs, and the possible surfactant effect for GaSb may not be operating any more.

As summarized in Table I, for sample C, the average distance of the interface dislocations almost coincide with the theoretical value of 5.51 nm for the GaSb/GaAs heterostructure, indicative of a relaxed (99.6%) epitaxial layer.[25] Consequently, if it was possible to tune the confinement of the misfit dislocation at the interface and to form a perfectly uniform Lomer dislocation array, this may lead to the growth with smooth surfaces and a dramatic reduction in the threading dislocations density in the epitaxial layers.[17,21]

In the following we try to determine the atomic type and arrangement of these interface dislocations. To this end, we apply the GPA of HRTEM (Refs. 26 and 27) to investigate the local strain distribution which characterizes the dislocation cores. Figure 6 shows the ε_{xx} component of the strain field (deformation along the [001] growth direction) derived from Fig. 4. On these images the dislocation cores are easily delineated at the nanometer scale: they correspond to the areas where the strain is maximal. Besides the strain distribution, for the two samples (A and B), all the Lomer dislocation cores are split in two [Figs. 6(a) and 6(b)]. Now moving to samples C and D, it can be noticed in Fig. 7 that the cores of the Lomer dislocations are more compact, and this effect is more underlined in sample C. Moreover, the strain distributions in both images are more uniform, in contrast to the maps of Fig. 6. Projecting the strains on the growth direction allows to calculate the average value which can be related to the relaxation state of the layers. As shown in Figs. 6(b), 6(d), 7(b), and 7(d), the strain state of the four samples is quite different. For sample A, without AlSb, we have the largest strain state, with only 6.6% of the misfit that has been locally relieved, and as shown, for sample C, the relaxation of the 7.8% mismatch appears to have been attained, at least locally. These profiles provide an idea of the thickness of the highly strain interfacial layer thickness. The change in the intensity at the interface region reveals that the thickness of the dislocation cores region is 2.12 nm, 2.02 nm, 0.7 nm, and 1.14 nm for sample A, B, C, and D, respectively, as summarized in Table I.

The fine structure of the interface dislocation can further be analyzed using the method proposed by Kret *et al.*,[28,29] as based on the GPA technique. Indeed, the Burgers vector can be directly calculated from the strain field $\boldsymbol{\varepsilon}(x, y)$ obtained by GPA, and the components of its spatial distribution α_{13} and α_{23} are from the derivatives of the strain tensor as follows:[28]

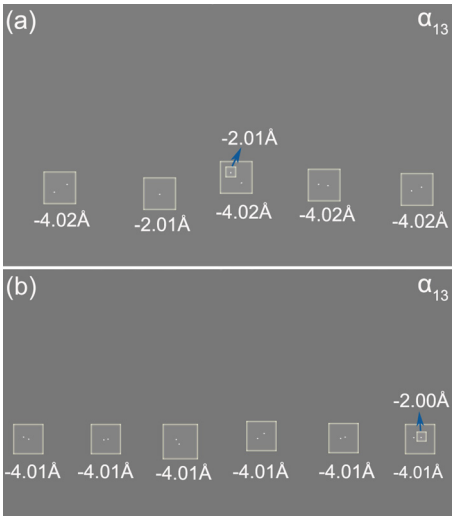

FIG. 8. (Color online) The α_{13} component of the dislocation distribution tensor field, the calculated Burgers vactors have been written in the image: (a) for sample B and (b) Sample C.

$$\alpha_{13} = -\frac{\partial \varepsilon_{xy}}{\partial x} + \frac{\partial \varepsilon_{xx}}{\partial y},$$

$$\alpha_{23} = -\frac{\partial \varepsilon_{yy}}{\partial x} + \frac{\partial \varepsilon_{yx}}{\partial y}.$$

The in-plane components of the tensorial field of the Burgers vector distribution take zero values over the whole region except at the dislocation cores, where they form local peaks. Such peaks are surrounded by a zero-field within an accuracy of 10^{-6} times the densities reached at the core position.[28]

Integrating the components of $\boldsymbol{\alpha}$ over the dislocation core region, we can obtain the components of the Burgers vectors as presented in Fig. 8, where it can be seen that the calculated Burgers vector components are very close to the theoretical value for Lomer dislocation (b=a/2[−110] =4.00 Å). Integrating the two dislocation density peaks of the Lomer dislocation separately, we obtain two Burgers vectors corresponding to in-plane components of two 60° dislocations. Therefore, in the analyzed areas, each Lomer dislocation is separated by a nanometer scale distance in two 60° dislocations, as shown by the core positions. The distance between dissociated cores for the Lomer dislocations as determined in many areas (more than 30 pairs of dislocations for each sample) is presented in Fig. 9. Obviously, the dislocation cores of sample C are more localized, indeed, the splittings are within 1 nm. For comparison of the four samples, we arbitrarily assume the interface dislocation is a Lomer, when the separation distance between the pairs of 60° dislocation is less than 1.5 nm. We then have 64.7%, 68.4%, 100%, and 75.8% of Lomer dislocations, for sample A, B, C, and D, respectively. Of course, this is a simple assumption, and for the four samples, all the interface dislocations are split into pairs of 60°; even in sample C, the pairs are indeed the closest but they are not completely merged.

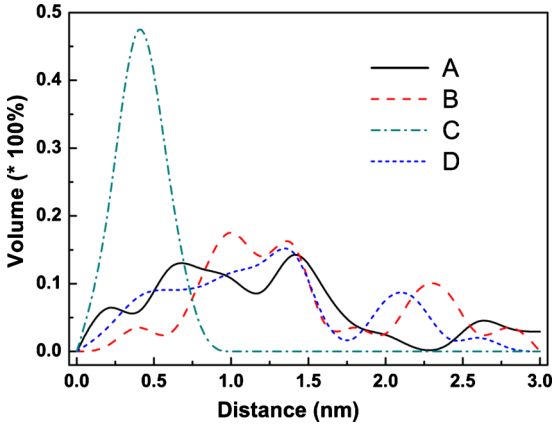

FIG. 9. (Color online) Statistical distribution of the distance between the 60° dislocation pairs of split Lomer dislocation cores.

IV. DISCUSSION AND CONCLUSION

From the above local analysis of the strain relief at the interfaces, it comes out that the AlSb interlayers thickness and the GaAs surface preparation are important parameters in determining the relaxation state of at the GaSb/GaAs interface. In their investigation, Kim *et al.*[21] have analyzed 1.2 nm, 9.7 nm, and 22 nm AlSb interlayer thicknesses. They reported that the smallest roughness and best interface structure was connected with the smallest AlSb interlayer (1.2 nm). This could be compared to our sample B and C. From these samples, we show that besides the AlSb thickness the surface preparation plays a crucial role. Indeed, comparison of samples A, B, and D evidences that the best results starting with an element III-rich GaAs surface are obtained for the thickest AlSb deposit. However, starting the AlSb growth on a Sb-rich GaAs surface (sample C) leads to even better results. This sample exhibits a relief of the local strain to mostly 100%, the interface dislocations as observed are all of Lomer type within our arbitrarily defined distance between the 60° dislocation pairs. Moreover, the interface thickness of this sample is the smallest, meaning that the strain is highly localized at the interface. One important point needs to be noticed at this stage, looking at the threading dislocation densities, our measured values are, of course, one order of magnitude lower than the other samples. Indeed, this is still two orders of magnitude higher than the best values reported in such systems,[3,15] which were reported to exhibit substantially low threading dislocation densities ($\sim 10^5$ cm^{-2}). If we look at the Burgers vectors distribution (Fig. 9), it is clear that even in our best sample, the large majority of the Lomer dislocations are still non merged 60° pairs, although quite close in distance. Then increasing the thickness to 16 ML (5 nm), the interface stays flat but the distance between the 60° pairs of interface dislocations is more fluctuating. So from the above observations, one may conclude that the decrease in the threading dislocations densities inside such highly mismatched compounds is possible to bring about following two procedures: (1) the formation of Lomer dislocations at the interface and (2) The localization of the strain inside the interface plane. The two processes will possibly be accompanied or lead to the formation of a flat interface. In the above observations, it is seen that flat

interfaces within 1 ML are attained for the two samples (C and D). For sample C, the distance between the pairs of 60° dislocation is less than 1 nm, whereas it fluctuates more in samples D, and the interface thickness also degrades.

From the reports on stress relaxation inside epitaxial layers, the glide of 60° dislocations to interface and reaction in pairs to form Lomer dislocations optimally contributes to the relaxation.[6] Inside investigated layers, the formation of nonmerged 60° dislocations with distances of 0.5–2 nm is observed to be systematic. In fact looking at the reports in the literature,[3,23] this behavior is probably not limited to our system and/or growth conditions, however further investigation is necessary in order to ascertain the role of these interfacial 60° pairs on the generation of the threading dislocations. Of course an important trend may be pointed out from our results; one order of magnitude reduction in threading dislocation density appears to be related to an increased localization of the strain at the interface, as well as, to the smallest splitting of the interface Lomer dislocations. These results may shine new insight on possible ways of optimization of the growth conditions for producing better quality GaSb layers. However, we have not yet attained substantially low threading dislocation densities as reported upon direct growth of GaSb on the GaAs substrate,[22] this result may be understood in the light of the observed systematic splitting of Lomer dislocations into 60° dislocations pairs and the fact that the local residual strain may depend on the position.

ACKNOWLEDGMENTS

This work is supported by the National Research Agency under Project MOS35, Contract No. ANR-08-NANO-022 and Project MICATEC, Contract No. ANR-07-NANO-049. Dr. S. Kret is gratefully acknowledged for his contribution to this work.

[1]I. Vurgaftman, J. R. Meyer, and L. R. Ram-Mohan, J. Appl. Phys. **89**, 5815 (2001).
[2]B. R. Bennett, R. Magno, J. B. Boos, W. Kruppa, and M. G. Ancona, Solid-State Electron. **49**, 1875 (2005).
[3]S. Huang, G. Balakrishnan, and D. L. Huffaker, J. Appl. Phys. **105**, 103104 (2009).
[4]A. Vila, A. Cornet, J. R. Morante, and P. Ruterana, Inst. Phys. Conf. Ser. **134**, 353 (1993).
[5]K.-N. Tu, J. W. Mayer, and L. C. Feldman, *Electronic Thin Film Science: For Electrical Engineer and Materials Scientist* (Macmillan, New York, 1992).
[6]P. M. J. Marée, J. C. Barbour, J. F. van der Veen, K. L. Kavanagh, C. W. T. Bulle-Lieuwma, and M. P. A. Viegers, J. Appl. Phys. **62**, 4413 (1987).
[7]A. Vila, A. Cornet, J. R. Morante, P. Ruterana, R. Bonnet, and M. Loubradou, Inst. Phys. Conf. Ser. **146**, 83 (1995).
[8]A. Georgakilas, P. Panayotatos, J. Stoemenos, J.-L. Mourrain, and A. Christou, J. Appl. Phys. **71**, 2679 (1992).
[9]A. Vilà, A. Cornet, J. R. Morante, P. Ruterana, M. Loubradou, R. Bonnet, Y. Gonzalez, and L. Gonzalez, Philos. Mag. A **71**, 85 (1995).
[10]W. Qian, M. Skowronski, R. Kaspi, M. De Graef, and V. P. Dravid, J. Appl. Phys. **81**, 7268 (1997).
[11]A. Vilà, A. Cornet, J. R. Morante, P. Ruterana, M. Loubradou, and R. Bonnet, J. Appl. Phys. **79**, 676 (1996).
[12]R. E. Mallard, P. R. Wilshaw, N. J. Mason, P. J. Walker, and G. R. Booker, Inst. Phys. Conf. Ser. **100**, 331 (1989).
[13]J.-H. Kim, T.-Y. Seong, N. J. Mason, and P. J. Walker, J. Electron. Mater. **27**, 466 (1998).
[14]W. Qian, M. Skowronski, and R. Kaspi, J. Electrochem. Soc. **144**, 1430 (1997).
[15]S. H. Huang, G. Balakrishnan, A. Khoshakhlagh, A. Jallipalli, L. R. Dawson, and D. L. Huffaker, Appl. Phys. Lett. **88**, 131911 (2006).
[16]J. M. Yarborough, Y.-Y. Lai, Y. Kaneda, J. Hader, J. V. Moloney, T. J. Rotter, G. Balakrishnan, C. Hains, D. Huffaker, S. W. Koch, and R. Bedford, Appl. Phys. Lett. **95**, 081112 (2009).
[17]K. Akahane, N. Yamamoto, S.-I. Gozu, A. Ueta, and N. Ohtani, J. Cryst. Growth **264**, 21 (2004).
[18]Y. H. Kim, J. Y. Lee, Y. G. Noh, M. D. Kim, S. M. Cho, Y. J. Kwon, and J. E. Oh, Appl. Phys. Lett. **88**, 241907 (2006).
[19]Y. H. Kim, Y. K. Noh, M. D. Kim, J. E. Oh, and K. S. Chung, Thin Solid Films **518**, 2280 (2010).
[20]S. J. Brown, M. P. Grimshaw, D. A. Ritchie, and G. A. C. Jones, Appl. Phys. Lett. **69**, 1468 (1996).
[21]H. S. Kim, Y. K. Noh, M. D. Kim, Y. J. Kwon, J. E. Oh, Y. H. Kim, J. Y. Lee, S. G. Kim, and K. S. Chung, J. Cryst. Growth **301–302**, 230 (2007).
[22]S. H. Huang, G. Balakrishnan, M. Mehta, A. Khoshakhlagh, L. R. Dawson, and D. L. Huffaker, Appl. Phys. Lett. **90**, 161902 (2007).
[23]B. R. Bennett, P. M. Thibado, M. E. Twigg, E. R. Glaser, R. Magno, B. V. Shanabrook, and L. J. Whitman, J. Vac. Sci. Technol. B **14**, 2195 (1996).
[24]A. Rocher and E. Snoeck, Mater. Sci. Eng., B **67**, 62 (1999).
[25]M. O. Manasreh, *Antimonide Related Strained Layer Heterostructures* (Gordon and Breach Science, Amsterdam, 1997), p. 107.
[26]M. J. Hÿtch, E. Snoek, and R. Kilaas, Ultramicroscopy **74**, 131 (1998).
[27]S. Kret, P. Ruterana, A. Rosenauer, and D. Gerthsen, Phys. Status Solidi B **227**, 247 (2001).
[28]S. Kret, P. Dluzewski, P. Dluzewski, and E. Sobczak, J. Phys.: Condens. Matter **12**, 10313 (2000).
[29]S. Kret, P. Ruterana, and G. Nouet, J. Phys.: Condens. Matter **12**, 10249 (2000).